HIV-PULSE: A long-read sequencing assay for high-throughput near full-length HIV-1 proviral genome characterization

Laurens Lambrechts[1,2], Noah Bonine[1,2], Rita Verstraeten[1,2], Marion Pardons[1], Ytse Noppe[1], Sofie Rutsaert[1], Filip Van Nieuwerburgh[3], Wim Van Criekinge[2], Basiel Cole[1#], Linos Vandekerckhove[1,#,*]

Affiliations

[1]HIV Cure Research Center, Department of Internal Medicine and Pediatrics, Ghent University Hospital, Ghent University, 9000 Ghent, Belgium.

[2]BioBix, Department of Data Analysis and Mathematical Modelling, Faculty of Bioscience Engineering, Ghent University, 9000 Ghent, Belgium.

[3]Laboratory of Pharmaceutical Biotechnology, Faculty of Pharmaceutical Sciences, Ghent University, 9000 Ghent, Belgium.

#These authors contributed equally

*Correspondence and requests for materials should be addressed to L.V. (email: linos.vandekerckhove@ugent.be)

Abstract

A deep understanding of the composition of the HIV-1 reservoir is necessary for the development of targeted therapies and the evaluation of curative efforts. However, current near full-length (NFL) HIV-1 proviral genome sequencing assays are based on labor-intensive and costly principles of repeated PCRs at limiting dilution, restricting their scalability. To address this, we developed a high-throughput, long-read sequencing assay called HIV-PULSE (HIV Proviral UMI-mediated Long-read Sequencing). This assay uses unique molecular identifiers (UMIs) to tag individual HIV-1 genomes, allowing for the omission of the limiting dilution step and enabling long-range PCR amplification of many NFL genomes in a single PCR reaction, while simultaneously overcoming poor single-read accuracy. We optimized the assay using HIV-infected cell lines and then applied it to blood samples from 18 individuals living with HIV on antiretroviral therapy, yielding a total of 1,308 distinct HIV-1 genomes. Benchmarking against the widely applied Full-Length Individual Proviral Sequencing assay revealed similar sensitivity (11% vs 18%) and overall good concordance, though at a significantly higher throughput. In conclusion, HIV-PULSE is a cost-efficient and scalable assay that allows for the characterization of the HIV-1 proviral landscape, making it an attractive method to study the HIV-1 reservoir composition and dynamics.

Introduction

The establishment of a viral reservoir shortly after HIV-1 infection leads to long-term viral persistence in people living with HIV-1 (PLWH) (1–3). While antiretroviral therapy (ART) can successfully suppress viral replication, it is not curative as the viral reservoir is not targeted (4, 5). Consequently, lifelong adherence to ART is required to prevent viral rebound, which usually takes place within several weeks following ART cessation (6). Despite the relatively low frequency of infected CD4 T cells that remain during ART (1/1,000 - 1/10,000), the size of the viral reservoir is remarkably stable, with an estimated half-life of 44 months (7, 8). The search for curative interventions targeting the viral reservoir remains one of the top priorities for achieving HIV-1 remission (9), however, this search is faced with two major challenges: (i) A lack of knowledge of the mechanisms governing HIV-1 latency and reservoir maintenance; (ii) A lack of high-throughput methods to measure the efficacy of reservoir-reducing interventions. To address these problems, technological advances that allow for a deep and high-throughput reservoir characterization are urgently needed (10).

Historically, the qualitative assessment of the HIV-1 reservoir has been carried out using two main types of assays: (i) Viral outgrowth assays (VOA), in which replication-competent viruses are reactivated and propagated ex vivo at limiting dilution, followed by quantification and sequencing of the cultured viral genomes (11, 12); (ii) Sequencing-based assays, where single proviral genomes are PCR-amplified from bulk DNA at limiting dilution, followed by Sanger- or short-read next-generation sequencing (NGS) (13–19). The VOA-based methods have the inherent benefit that they focus on replication-competent viruses, though they are usually long, costly and labor-intensive and have been shown to underestimate the true size of the replication-competent fraction following one round of reactivation (15). Sequencing-based methods allow the assessment of a small subgenomic region of interest or the near full-length (NFL) proviral genome (~90%) (13–19). In the case of the latter, the percentage of genome-intact proviruses can be derived, which has previously been estimated at 2-5% on average (16). More recently, several flow-cytometry-based assays have been developed to

isolate and study HIV-infected cells harboring an inducible provirus such as Simultaneous TCR, Integration site and Provirus sequencing (STIP-Seq), which specifically targets the translation-competent reservoir (20–22). In these assays, the infected cells are dispensed into single wells of a microtiter plate, followed by genomic or transcriptomic sequencing.

A common denominator of the assays described above is that they all rely on the physical isolation of individual viral genomes into different wells of a microtiter plate, followed by the PCR amplification of each genome in separate reactions (23). This principle is both labor-intensive and costly, severely limiting the applicability in large scale projects.

Up until the advent of long-read sequencing technologies, long amplicons (>5 kb) were either sequenced by a series of overlapping Sanger sequencing reactions, or by fragmentation of the amplicon into smaller pieces followed by short-read NGS (16–18). Long-read sequencing technologies offer the ability to sequence long amplicons in a single read, however, these technologies suffer from a high error rate of single-pass reads (~5-10%) (24). Recently, Karst et al. developed a protocol that uses unique molecular identifiers (UMIs) to obtain high-accuracy consensus sequences from long amplicons (>5 kb), overcoming the problem of the limited single-read accuracy (25).

Here, we present a new assay that allows for high-throughput amplicon sequencing of NFL HIV-1 genomes, called HIV-PULSE: HIV Proviral UMI-mediated Long-read Sequencing. By tagging individual HIV-1 genomes with two distinct UMIs, the step of limiting dilution can be omitted, enabling the amplification of many NFL genomes in a single reaction (25). After optimization of the assay on HIV-infected cell lines, we used the protocol to characterize the viral reservoirs of a chronic cohort of PLWH on ART (n=18). Benchmarking against the widely used Full-Length Individual Proviral Sequencing (FLIPS) assay revealed comparable accuracy and efficiency, but a remarkably higher throughput and lower cost per sequenced NFL HIV-1 genome (17). In conclusion, HIV-PULSE is a valuable addition to the arsenal of HIV-1 proviral sequencing methods and opens new possibilities for investigating the composition and dynamics of the HIV-1 reservoir.

Materials and Methods

Biological Resources

Study participants and sample collection

A total of 18 individuals on suppressive ART were included in this study (Supplemental Table 1). Participants were recruited at Ghent University Hospital and donated blood samples. Some participants agreed to additional leukapheresis to harvest large amounts of leukocytes. Peripheral blood mononuclear cells (PBMCs) were isolated by Ficoll density gradient centrifugation and were cryopreserved in liquid nitrogen. CD4 T cells were isolated from PBMCs by negative selection using EasySep Human CD4 T Cell Enrichment Kit (StemCell Technology, #19052). All participants signed informed consent forms approved by the Ethics Committee of the Ghent University Hospital (Belgium) (Ethics Committee Registration number: 2015/0894, 2016/0457, BC-07056).

Cell lines

J-Lat 8.4 cells (ARP-9847, contributed by dr. Eric Verdin), a Jurkat-based cell line latently infected with HIV, and Jurkat E6.1 cells (ARP-177, contributed by dr. Arthur Weiss) were obtained through the NIH HIV Reagent Program, Division of AIDS, NIAID, NIH (26, 27). J-Lat and Jurkat cells were grown in RPMI1640 (Gibco, #11875093) supplemented with 10% fetal bovine serum (HyClone, #RB35947) and 1% Pen/Strep (Gibco, #15140122).

DNA isolation and HIV-1 DNA reservoir size measurement

Genomic DNA from pelleted cells was isolated via column extraction using the DNeasy Blood & Tissue Kit (Qiagen, #69506) according to the manufacturer's instructions. The DNA concentration of each extract was measured on a Qubit 3.0 fluorometer using the Qubit dsDNA BR assay kit (ThermoFisher Scientific, #Q32853). The HIV-1 copy number was determined by a total HIV-1 DNA assay on droplet digital PCR (Bio-Rad, QX200 system), as described previously (28). PCR amplification was carried out with the following cycling program: 10 m at 95°C; 40 cycles (30 s at 95°C, 1 m at 56°C); 10 m at 98°C. Droplets were

read on a QX200 droplet reader (Bio-Rad). Analysis was performed using ddpcRquant software (29).

Full-length individual proviral sequencing

The full-length individual proviral sequencing (FLIPS) assay was performed as described by Hiener et al. (17). A detailed protocol can be found on the following link: dx.doi.org/10.3791/58016. In short, genomic DNA was used as input for a nested PCR performed at an endpoint dilution where <30% of the reactions are positive. The cycling conditions were 94°C for 2 m; then 94°C for 30 s, 64°C for 30 s, 68°C for 10 m for 3 cycles; 94°C for 30 s, 61°C for 30 s, 68°C for 10 m for 3 cycles; 94°C for 30 s, 58°C for 30 s, 68°C for 10 m for 3 cycles; 94°C for 30 s, 55°C for 30 s, 68°C for 10 m for 21 cycles; then 68°C for 10 m. For the second round, 10 extra cycles at 55°C were included. The PCR products were visualized using agarose gel electrophoresis (1% agarose gel). Proviral amplicons from positive wells were cleaned using AMPure XP beads (Beckman Coulter, #A63880), followed by a quantification of each cleaned provirus with Quant-iT PicoGreen dsDNA Assay Kit (Invitrogen, #P11496).

Illumina short-read sequencing

Selected FLIPS proviral amplicons underwent NGS library preparation using the Nextera XT DNA Library Preparation Kit (Illumina, #FC-131-1096) with indexing of 96-samples per run according to the manufacturer's instructions (Illumina, #FC-131-2001), except that input and reagents volumes were halved and libraries were normalized manually. The pooled library was sequenced on a MiSeq Illumina platform via 2x150 nt paired-end sequencing using the 300 cycle v2 kit (Illumina, #MS-102-2002).

HIV-PULSE assay methodology

Pre-amplification

A first PCR was used to specifically target and pre-amplify HIV-1 proviral templates using the outer primers of a nested HIV-1 primer set (listed in Supplemental Table 2, Figure 1A). Each PCR reaction contained 500 ng of genomic DNA, 2 µL LongAmp Taq DNA Polymerase

(NEB, # M0323L), 0.5 µM of each primer (First PCR F, First PCR R), 1.5 µL 10 mM dNTPs (Promega, #C1141), 10 µL 5X LongAmp Taq Reaction Buffer in 50 µL. The following cycling conditions were used: 94°C for 1 m 15 s; then 94°C for 30 s, 63°C for 30 s, 65°C for 10 m for 6 cycles; then 65°C for 10 m. The number of amplification cycles can be reduced to 5 cycles for samples from individuals with a high reservoir size (>2,500 total HIV-1 DNA copies/million CD4) to prevent overbinning. PCR products were cleaned using CleanPCR magnetic beads (CleanNA, #CPCR-0050) at a 1.0x beads/sample ratio.

Tagging HIV-1 templates

A second PCR was performed to tag both ends of the pre-amplified proviral HIV-1 templates with a tailed UMI (listed in Supplemental Table 2). Primers were designed to contain: (i) a synthetic primer binding site used in later stages for amplification, (ii) a UMI with a repetitive pattern of 12 random nucleotides and 6 degenerate nucleotides (Y/R) and (iii) an HIV-1 inner primer of the nested primer set to target the pre-amplified templates (Figure 1A, Supplemental Figure 1A). Each PCR reaction contained all the cleaned pre-amplified product (30 µL), 2 µL LongAmp Taq DNA Polymerase (NEB, # M0323L), 0.5 µM of each primer (Second PCR F UMI, Second PCR R UMI), 1.5 µL 10 mM dNTPs (Promega, #C1141), 10 µL 5X LongAmp Taq Reaction Buffer in 50 µL. The following cycling conditions were used: 94°C for 1 m 15 s; then 94°C for 30 s, 58°C for 30 s, 65°C for 10 m for 2 cycles; then 65°C for 10 m. Tagged PCR products were cleaned using CleanPCR magnetic beads (CleanNA, #CPCR-0050) in a custom buffer solution (based on the 'SPRI size selection protocol for >1.5–2 kb DNA fragments' protocol provided by Oxford Nanopore Technologies (ONT)) at a 0.9x beads/sample ratio and eluted in 30 µL nuclease-free water (NFW).

Amplification of UMI-tagged proviruses

The next steps used 4 consecutive PCR amplification rounds of each 10 cycles followed by a clean up to produce enough template input required for long-read sequencing while preserving amplicon size distributions. Here, we made use of a primer set that binds to the

synthetic binding site incorporated during the previous tagging stage. The PCR mix consists of 2 µL LongAmp Taq DNA Polymerase (NEB, # M0323L), 0.5 µM of each primer (ncec_pcr_fw_v7, ncec_pcr_rv_v7), 1.5 µL 10 mM dNTPs (Promega, #C1141), 10 µL 5X LongAmp Taq Reaction Buffer in 50 µL. For the first PCR amplification round all the cleaned tagging products from the previous step (30 µL) were used as template input while during the second, third and fourth amplification rounds only a third of the cleaned product of the previous round is used (10 µL). The following cycling conditions were used: 94°C for 1 m 15 s; then 94°C for 30 s, 58°C for 30 s, 65°C for 10 m for 2 cycles; then 65°C for 10 m. PCR products were cleaned after each consecutive round using regular CleanPCR magnetic beads (CleanNA, #CPCR-0050) at a 1.0x beads/sample ratio and eluted in 30 µL NFW. During the last round of 10 cycles, the regular primers were switched for a custom set of tailed primers to barcode the PCR products from the same participant with a specific, identical identifier (listed in Supplemental Table S2). After the last PCR round, the end products were visualized using agarose gel electrophoresis (1% agarose gel) and the DNA concentration was determined using a Qubit 3.0 fluorometer with the Qubit dsDNA BR assay kit (ThermoFisher Scientific, #Q32853).

ONT long-read sequencing

Samples were multiplexed using the Native Barcoding Kit (ONT, #EXP-NBD104) using the following strategy: each PCR replicate was assigned to a different ONT barcode and contained equimolarly pooled PCR products from different participants. In later stages, this allows to assign reads to the correct PCR replicate by the ligated ONT barcode and to the correct sample by the participant-specific identifier attached during the last PCR round (Supplemental Figure 1A). For library preparation, the Ligation Sequencing Kit (ONT, #SQK-LSK109) was used following the manufacturer's instructions. Samples were sequenced on a MinION ONT device using MinION R10.3 flow cells and the MinKNOW v21.02.1 software followed by basecalling at super accuracy mode and demultiplexing with Guppy v5.0.17.

Bioinformatics analysis of long-read data

196 For the analysis of long-read data, a customized version of the UMI data analysis workflow
197 as described by Karst et al. was utilized (Supplemental Figure 1B) (25). The adapted scripts
198 can be found at https://github.com/laulambr/longread_umi_hiv, main changes include
199 updated software versions of samtools (1.11), medaka (1.4.3) and racon (1.4.20). Before the
200 data was analyzed using the UMI pipeline, the demultiplexed ONT reads were first mapped
201 against the HXB2 reference sequence using minimap2 (2.17) to filter out non-HIV-1 reads.
202 Next, the '*longread_umi nanopore_pipeline*' workflow was run separately on each replicate
203 read dataset using the following settings: *-s 200 -e 200 -m 1500 -M 10000 -f*
204 *CAAGCAGAAGACGGCATACGAGAT -F AAGTAGTGTGTGCCCGTCTGTTGTGTGAC -r*
205 *AATGATACGGCGACCACCGAGATC -R GGAAAGTCCCCAGCGGAAAGTCCCTTGTAG -c*
206 *3 -p 1 -q r103_hac_g507 -U 'r103_min_high_g360'*. The workflow consists of the following
207 consecutive steps; (i) trimming and filtering of the HIV-1 long-read sequencing data using
208 Porechop (v.0.2.4, https://github.com/rrwick/Porechop), Filtlong (v.0.2.0,
209 https://github.com/rrwick/Filtlong) and cutadapt (v.2.7) (30), (ii) extraction of UMI reference
210 sequences using cutadapt (v.2.7) and usearch (30, 31), (iii) binning of reads to UMI
211 combinations using bwa (v0.7.17) and samtools (v1.11) while excluding chimeric artifacts,
212 (iv) generation of bin consensus sequences using usearch and minimap2 (v2.17) (31, 32)
213 and (v) polishing of bin consensus data by multiple rounds of racon (v.1.4.20) and a final
214 round of Medaka (v.1.4.3, https://github.com/nanoporetech/medaka) (33).

215 Next, a custom bioinformatics workflow specific to the HIV-PULSE protocol was run to
216 correct for pre-amplification, improve final consensus accuracy and evaluate clonality among
217 PCR replicates. First, the polished bin consensus sequences from each replicate dataset
218 were demultiplexed to their respective participant using the '*longread_umi demultiplex*'
219 workflow. For each participant, bin consensus sequences from all PCR replicates were
220 pooled together and screened for the occurrence of identical UMIs. Identical UMI pairs in
221 different PCR replicates are technically not possible but these artifacts may arise due to
222 misassignment during the initial raw ONT reads demultiplexing by Guppy. In these cases,

the bin in the replicate with the highest coverage was considered correct while the others were removed from their respective replicate datasets. As the assay relies on a pre-amplification phase, single proviral templates will have been amplified and potentially tagged into bins with different UMI pairs. This prohibits the screening for clonal proviruses present in one bulk PCR reaction as pre-amplification would also lead to the presence of identical proviruses in bins with different UMI pairs. To correct for this, identical proviruses (due to clonality or pre-amplification) present in the bin consensus sequences from each participant were identified by clustering genomes with similar sizes and >99.5 % sequence identity into a megabin using usearch (31). For megabins consisting of >3 bins, a new consensus sequence was constructed to help to resolve remaining errors. For megabins that only consisted of 2 bin consensus sequences, the bin with the highest coverage (~accuracy) was retained while bins that did not cluster remained as unique bins. Finally, an assessment of clonality among different PCR replicates was made by screening the resulting megabins for the presence of bin sequences originating from different PCR replicates. If the same proviral sequence was found in multiple PCR replicates, it is considered as evidence of a potential clonal origin, as opposed to proviruses that are only found in one replicate. By performing multiple PCR replicates, one can identify clonal populations, however, accurate quantification of reservoir clonality is hindered by the fact that identical proviruses found within the same PCR replicate are collapsed and counted as one (to exclude potential bias by pre-amplification).

Bioinformatics analysis of Illumina data

NFL genome sequences derived from FLIPS reactions were de novo assembled as follows: (i) FASTQ quality checks were performed with FastQC v0.11.7 (http://www.bioinformatics.babraham.ac.uk/projects/fastqc) and removal of Illumina adaptor sequences and quality-trimming of 5′ and 3′ terminal ends was performed with bbmap v37.99 (https://sourceforge.net/projects/bbmap/). (ii) Trimmed reads were de novo assembled using MEGAHIT v1.2.9 with standard settings (34). (iii) Resulting contigs were

aligned against the HXB2 HIV-1 reference genome using blastn v2.7.1 with standard settings, and contigs that matched HXB2 were retained (35). (iv) Trimmed reads were mapped against the *de novo* assembled HIV-1 contigs to generate final consensus sequences based on per-base majority consensus calling, using bbmap v37.99 (https://sourceforge.net/projects/bbmap/). Scripts concerning de novo assembly of HIV-1 genomes can be found at the following GitHub page: https://github.com/laulambr/virus_assembly.

HIV-1 genome classification

NFL proviral genome classification was performed using the publicly available "Gene Cutter" and "Hypermut" webtools from the Los Alamos National Laboratory HIV sequence database (https://www.hiv.lanl.gov). Proviral genomes were classified in the following sequential order: (i) "Inversion": presence of internal sequence inversion, defined as region of reverse complementarity. (ii) "Large internal deletion": internal sequence deletion of >1000 bp. (iii) "Hypermutated": APOBEC-3G/3F-induced hypermutation. (iv) "packaging signal and/or major splice donor (PSI/MSD) defect": deletion >7 bp covering (part of) the packaging signal region or absence of GT dinucleotide at the MSD and GT dinucleotide at the cryptic donor site (located 4 bp downstream of MSD) (19). Proviruses with a deletion covering PSI/MSD that extended into the *gag* gene, thereby removing the *gag* AUG start codon, were also classified into this category. (v) "Premature stop-codon/frameshift": premature stop-codon or frameshift caused by mutation and/or sequence insertion/deletion in the essential genes *gag*, *pol* or *env*. Proviruses with insertion/deletion >49 nt in *gag*, insertion/deletion >49 nt in *pol*, or insertion/deletion >99 nt in *env* were also classified into this category. (vi) "Intact": proviruses that displayed none of the above defects were classified into this category.

Reference sequences

Proviral HIV-1 genomes from participants previously acquired with the FLIPS and STIP-Seq assays in the context of former studies were included as references (20). Accuracy metrics on the new HIV-PULSE assay compared to FLIPS and STIP-Seq reference proviruses (sequenced using Illumina technology) were calculated using pomoxis (v0.3.6, https://github.com/nanoporetech/pomoxis).

Phylogenetic analysis

Sequences obtained with the HIV-PULSE assay, STIP-Seq and FLIPS were multiple aligned using MAFFT (v 7.471) (36). DIVEIN was used to calculate pairwise diversity among proviral sequences (37). Phylogenetic trees were constructed using PhyML v3.0 (best of NNI and SPR rearrangements) and 1,000 bootstraps (38). R (v4.1.2), ggplot (v3.3.5) and ggtree (v3.2.1) were used for visualization and annotation of trees (39–41).

Results

Optimization of PCR cycling conditions on HIV-infected cell lines

Since the frequency of HIV-1 infected cells in ART-suppressed PLWH is remarkably low, typically in the range of 100-1,000 proviral genomes per million CD4 T cells, we set out to devise an assay allowing for the detection of such rare events using a UMI-binning strategy (Figure 1A) (7). By including a pre-amplification step, the sensitivity of the assay should considerably improve as more target templates are created, thus increasing the number of tagged templates transferred to the PCR amplification step. This hypothesis was tested by preparing a dilution series of J-Lat 8.4 DNA (HIV-infected CD4 T cell line) in Jurkat DNA (non-infected parental CD4 T cell line). The dilution series, ranging from 100% to 0.01% J-Lat 8.4 DNA (Jurkat as negative control), was subjected to either 0, 2, 4, 6 or 8 cycles of pre-amplification, using primers that target NFL HIV-1 (Figure 1B). Each amplification was performed in triplicate, using a fixed input of 500 ng genomic DNA (corresponding with ~82,500 CD4 T cells) with the PCR success being determined by visualization of the ~9.5 kb amplicon by agarose gel electrophoresis. As expected, reactions with an input of undiluted J-Lat DNA were all successful regardless of the number of pre-amplification cycles (Figure 1B). However, in samples with a proviral burden closer to those observed in samples from PLWH (~0.1%) at least 6 cycles of pre-amplification were required for guaranteed PCR success.

Next, we set out to determine whether high-accuracy HIV-1 genomes could be acquired by performing long-read sequencing of the J-Lat 8.4 PCR products and subsequent analysis using a custom version of the UMI pipeline developed by Karst et al. (25). Using an ONT R10.3 flow cell, reads with a median length of 9.5 kb were generated, in agreement with the expected amplicon length of J-Lat 8.4 DNA (Supplemental Figure 1C-H). The bioinformatics pipeline allowed for the construction of the UMI-tagged proviruses by binning the reads based on the observed terminal UMI pairs in the sequencing data (Figure 1A). During these steps, non-HIV reads were filtered out (removing non-specific amplicons) and aberrant UMI

bins not meeting a fixed list of criteria (*e.g.* chimeras, read orientation bias) were excluded (Supplemental Figure 1B-H, for LIB01 (sequencing library containing the J-Lat 8.4 amplicon reads) ~30% of all detected UMI pairs did not meet the criteria, however, they accounted only for 16% of all the binned reads). For each bin, a consensus sequence was constructed by multiple rounds of polishing (racon, medaka) of the assigned raw reads. To assess the accuracy of the proviral UMI consensus sequences, we compared each bin to a reference genome of the J-Lat 8.4 amplicon sequenced with Illumina. As more reads were assigned to a bin, an increase in the mean accuracy could be observed before reaching a plateau at 99.9% (Figure 1C). Bins with a coverage of at least 15 reads passed the Q30 (99.9% accuracy) threshold. At the Q30 threshold, an average of 8 mismatches per 9.5 kb genome could be observed, while aberrant deletions and insertions were completely resolved (Figure 1D).

Application of the assay on samples from PLWH and comparison to FLIPS

To assess the performance of the HIV-PULSE assay on samples from ART-suppressed PLWH, and to benchmark it to a gold standard short-read sequencing assay, DNA from peripheral blood CD4 T cells from 4 individuals was subjected to both the HIV-PULSE and the FLIPS assay (Figure 2). This yielded a median of 18 FLIPS and 87 HIV-PULSE distinct proviruses per participant (Figure 2A and Supplemental Figure 2). Of note, in the case of FLIPS, 10 out of 136 HIV-1 PCR amplicons failed to produce a correct HIV-1 genome during *de novo* assembly (Supplemental Figure 2A, median of 2.5 assembly failures per participant). Across both assays, a total of 16 overlapping expansions of identical sequences (EIS) were observed (Figure 2A). HIV-PULSE successfully identified 81% (13/16) of the overlapping EIS as being clonal, while FLIPS detected 37.5% of the EIS (6/16). However, this discrepancy is probably the result of the lower number of genomes assayed with FLIPS (~5-fold). We compared the overlapping proviral sequences to estimate sequencing accuracy and link it to proviral classification. The mean accuracy was found to be 99.99% (Q40) for the megabinned proviruses, with residual errors observed in only four genomes

due to homopolymeric regions (Supplemental Figures 2B-C). However, these errors did not affect the correct HIV-1 proviral classification.

Overall, comparing HIV-PULSE results to FLIPS data reveals (i) No significant differences between the proportions of sampled unique proviruses with each assay (Figure 2A; p=1.00, p=0.583, p=1.00, p=1.00 for P03, P12_T1, P12_T2 and P14, respectively) and (ii) No significant bias in the size distribution of the observed proviral genome lengths (Figure 2B, median lengths are 4,620 for HIV-PULSE and 4,531 for FLIPS, p=0.0810). The efficiency of both methods was assessed by calculating the percentage of total detected proviruses out of the total HIV-1 DNA reservoir size (Figure 2C). Slightly lower efficiencies were observed with the HIV-PULSE assay (mean of 11% opposed to 18% with FLIPS, p=0.271), however, this measure is likely an underestimation as it does not account for clonality of the reservoir (true size of clones is missed).

In conclusion, these results indicate that HIV-PULSE displays the required sensitivity for the amplification of NFL HIV-1 genomes from samples of ART-suppressed PLWH. Furthermore, both the accuracy and efficiency of the assay are on par with the FLIPS assay.

HIV-PULSE enables high-throughput sequencing of NFL genomes in a large cohort of PLWH

The assay was next applied to peripheral blood CD4 T cell DNA of 18 chronically treated PLWH (mean time on ART = 11.2 years, Supplemental Table 1). The HIV-PULSE assay yielded an average of 15 ± 3 distinct HIV-1 proviruses per replicate, per participant (range: 3-55). For each participant, a mean PCR success rate of 97% was observed among the 6 PCR replicates based on agarose gel visualization (Supplemental Table 3). Overall, a total number of 1,661 proviruses (1,308 distinct) were retrieved across all participants (mean of 87 HIV-1 proviruses per sample, Supplemental Table 3, Supplemental Figure 3). Excluding the effect of clonal proliferation on infected cells, we looked at the presence of putatively intact genomes within the 1,308 distinct proviruses. A mean proportion of 5% intact distinct

366 genomes was found across the 19 samples, which corresponds to previously reported
367 numbers (Figure 3A) (16–18). Putatively intact sequences found across multiple replicates,
368 indicative of clonality, were seen in 9/14 participants with at least 1 distinct intact sequence
369 (Figure 3B). As two collected samples belonged to the same individual (P12) taken 3 years
370 apart, a longitudinal assessment of the reservoir composition could be performed. This
371 revealed the persistence of 21 infected cell clones (two with an intact provirus) between the
372 two sampled timepoints (Figure 3, Supplemental Figure 4). No significant differences
373 were observed in both the yield (p=0.662, 19 at T1 vs 18 at T2 mean distinct viruses per
374 replicate, Figure 3A, Supplemental Table 2) and the observed mean pairwise distance
375 among intact sequences between the two timepoints (P12_T1: 0.0230 n=7 vs P12_T2:
376 0.0197, n=5).

377 While the characteristics of the cohort are quite diverse, we were still able to get a fair
378 number of proviral sequences in individuals with a low total HIV-1 reservoir size (<500 total
379 HIV DNA copies/million CD4, n=3). A significant correlation between the HIV-PULSE yield
380 and the reservoir size measured by total HIV DNA was observed (Supplemental Figure 5,
381 R=0.71, p=1.5*10^{15}). On average, the efficiency of HIV-PULSE for these samples was 13%
382 (95% CI [7.9, 17.6]) as calculated by dividing the number of detected distinct proviruses by
383 the total number of input HIV-1 copies per PCR replicate (Supplemental Table 3).
384 Nevertheless, this measure of efficiency is an underestimation, as it does not account for
385 clones found within a replicate.

386 **HIV-PULSE detects proviruses of the translation-competent HIV-1 reservoir**

387 While the proviral reservoir consists of a heterogeneous mix of HIV-1 proviruses belonging
388 to different classes, only a few can contribute to viral rebound and/or HIV-1 pathogenesis by
389 inducing chronic immune activation (*e.g.* intact, PSI/MSD defect) (20, 42, 43). Of particular
390 clinical interest, the translation-competent HIV-1 reservoir represents all proviruses that can
391 produce viral proteins following maximal stimulation, consequently enriching for replication-
392 competent proviruses (42). In this regard, we next set out to evaluate whether HIV-PULSE

393 can capture proviruses that belong to the translation-competent reservoir, by comparing HIV-
394 PULSE data (n=8 participants) to STIP-Seq data (Figure 4A). On average per individual,
395 69% (95% CI [45, 92]) of the translation-competent STIP-Seq clones were detected with
396 HIV-PULSE (as unique or clone). This corresponds to a total of 17 overlaps among both
397 assays, of which 10/17 (59%) were also identified as a clone by HIV-PULSE, as they were
398 detected across multiple replicates from the same participant (Figure 4B). Additionally, 17
399 clones were found in the HIV-PULSE data but not sampled with STIP-Seq (6/17 intact),
400 which could be due to the integration of those proviruses at a chromosomal location in
401 regions with features (*e.g.* heterochromatin) associated with HIV-1 transcriptional latency or
402 a location less prone to be induced by latency reversing agents or by the more limited
403 number of proviruses assessed with STIP-Seq compared to HIV-PULSE (44, 45). In
404 conclusion, HIV-PULSE reliably picks up proviruses that belong to the translation-competent
405 reservoir, which is of high importance for applicability in a clinical setting.

Discussion

To achieve an HIV-1 cure, a comprehensive understanding of the persisting viral reservoir is crucial. Over the recent years, the application of HIV-1 NFL sequencing assays has increased our knowledge of certain key aspects, such as the proviral genomic composition and reservoir dynamics within PLWH. Still, all these results have been obtained through labor-intensive assays relying on limiting dilution and subsequent one-by-one sequencing of proviral genomes, limiting their application in large-scale studies. Here, we present the HIV-PULSE assay, allowing for a scalable, high-throughput assessment of the proviral HIV-1 reservoir. The use of dual barcodes removes the need for limiting dilution, allowing the amplification of multiple proviral HIV-1 templates during long-range NFL PCR on bulk DNA, while overcoming the inherently low single-read accuracy of long-read sequencing technologies. Benchmarking against the gold standard FLIPS method revealed comparable accuracy and efficiency, though notable differences in terms of throughput and associated costs are apparent. An overview of the approximated cost (in USD) per proviral sequence for each method indicates a 10-fold price reduction in favor of HIV-PULSE (Supplemental Table 4). Aside from a clear cost benefit, eliminating the limiting dilution step and sampling multiple proviruses out of a single PCR reaction offers a more high-throughput approach to NFL HIV-1 reservoir characterization. To illustrate, at least 52 96-well FLIPS PCR plates at limiting dilution would be required to obtain the equivalent of 1,661 total HIV-PULSE proviruses (Supplemental Table 4). Also, as a consequence of employing short-read NGS, FLIPS requires a *de novo* assembly step, which sometimes fails when resolving more complex genomes.

In this study, we applied HIV-PULSE to peripheral blood samples from a cohort of 18 PLWH on chronic ART, to study the composition of their HIV-1 viral reservoir. Out of the 1,308 distinct proviruses detected, ~5% were deemed genome-intact, agreeing with earlier reports on PLWH on chronic ART (16). We compared the HIV-PULSE assay to the STIP-Seq assay for 8 participants, showing that HIV-PULSE efficiently picked up translation-competent

proviruses, detecting 69% of the clonal sequences found with STIP-Seq. Interestingly, HIV-PULSE detected additional putatively intact proviral genomes which were not detected with the STIP-Seq assay, potentially representing hard-to-reactivate proviruses in a deep state of latency. While the HIV-PULSE assay does not enable a specific enrichment of the translation-competent reservoir, these findings make a case for HIV-PULSE as a tool to perform qualitative in-depth characterization of the functional reservoir dynamics in response to curative interventions during clinical trials. The high-throughput and cost-efficient nature of the HIV-PULSE assay makes it an attractive method for use within large-scale clinical studies of the HIV-1 reservoir with applications ranging from performing a longitudinal phylogenetic analysis of the proviral reservoir, screening multiple samples from the same individual for compartmentalization across different tissues, drug-resistance screening and bNAb epitope mapping. Indeed, implementing a qualitative NFL approach in clinical trial settings could help to check whether participants are eligible by excluding pre-existing resistance to a compound of interest or to assess immune escape following the intervention (46–48).

The adoption of long-read sequencing technologies for amplicon sequencing has historically been taken aback by the poor single-read accuracy. Notwithstanding these initial reservations, others have been developing long-read assays to characterize different aspects of the HIV-1 reservoir over the last couple of years. Pooled CRISPR Inverse PCR sequencing (PCIP-seq) allows to study both the integration site and the associated provirus using a targeted enrichment and inverse PCR strategy (49). While the collected data is certainly informative, the approach is hampered by limited sensitivity (3.2%), inadequate proviral coverage for accurate genome assembly and its reliance on the design of a custom pool of CRISPR guide RNAs for each participant. In comparison, HIV-PULSE has an improved sensitivity (13%), produces high-accuracy genomes, and does not rely on individualized primer designs, although information on the genomic location of the integrated provirus is missing. Another group developed NanoHIV, a bioinformatics tool to construct

460 HIV-1 consensus sequences from long-read ONT data (50). This follows a reference
461 mapping-based strategy with consecutive mappings to refine the original draft and deal with
462 variable genomic regions. To compare the performance, they generated consensus
463 genomes of NFL amplicons (acquired via nested NFL PCR performed at limiting dilution)
464 and performed sequencing with both ONT and NGS Illumina. The authors report a mean
465 accuracy of 99.4% (or 54 errors in a 9 kb genome), considerably lower than the megabin
466 accuracy of 99.99% (or 1 error in a 9 kb genome) reported with our bioinformatics pipeline.
467 Two studies describe protocols to amplify and sequence different genomic regions with
468 accuracies up to 99.9% from virions in plasma samples from viremic individuals. While one
469 relies on circular consensus sequencing (CSS) reads with PacBio technology to obtain 2.6
470 kb full-length *env* sequences (51), the other method Multi-read Hairpin Mediated Error-
471 Correction Reaction (MrHAMER) targets a 4.6 kb *gag-pol* region followed by sequencing on
472 a MinION ONT device (52). Despite showcasing great promise, the aforementioned
473 strategies have not been applied to the more challenging setting of HIV-1 reservoir, which
474 requires several orders of magnitude greater sensitivity.

475 We do acknowledge some limitations to this assay. First, the inclusion of the pre-
476 amplification step to ensure efficient tagging and enrichment impedes the accurate
477 quantification of reservoir clonality, as the dual UMI tags are only incorporated after the initial
478 pre-amplification cycles. However, by performing multiple PCR replicates, we were still able
479 to identify most clonal populations throughout this study. Further research into increasing the
480 efficiency of the UMI tagging step would be needed to omit the pre-amplification step.
481 Despite the limitations of HIV-PULSE in terms of accurate reservoir quantification, the assay
482 can be valuable in areas where quantification does not matter, such as the aforementioned
483 HIV-1 phylogenetics, drug resistance screening, and bNAb epitope mapping. Second, while
484 we cannot exclude the possibility of chimera formation during the initial pre-amplification
485 step, we consider it to be nearly impossible as chimera formation by PCR polymerase is
486 normally observed in reactions with high numbers of PCR cycles (53). Third, we successfully

applied the HIV-PULSE assay on samples from a chronic cohort of PLWH, yet samples from PLWH with different characteristics might be more challenging. As some steps of the analysis workflow rely on the sequence diversity to cluster identical bins into megabins to deconvolute the effect of pre-amplification, proviral reservoirs with lower intra-host sequence diversity (*e.g.* early ART initiation) could limit the success of this approach.

In conclusion, the HIV-PULSE assay presents itself as a promising HIV-1 NFL proviral sequencing method that enables scalable, high-throughput characterization of the proviral reservoir, while retaining sequencing accuracy comparable to HIV-1 NFL assays currently used in the field. We are convinced that the HIV-PULSE assay will be a valuable asset in advancing our understanding of the composition and dynamics of the viral reservoir during future basic and translational HIV-1 research.

Data Availability

HIV-1 proviral sequences are uploaded to GenBank (accession numbers pending for GenBank approval). Sequencing data has been submitted to Sequence Read Archive (SRA) under BioProject ID (will be made available upon publication). The bioinformatics pipeline is available at https://github.com/laulambr/longread_umi_hiv.

Funding

This current research work was supported by the NIH (R01-AI134419, MPI: L.V.) and the Research Foundation Flanders (S000319N and G0B3820N). L.V. was supported by the Research Foundation Flanders (1.8.020.09.N.00) and the Collen-Francqui Research Professor Mandate. The sample collection at UZ Ghent was supported by an MSD investigator grant (ISS 52777). B.C. and L.L. were supported by FWO Vlaanderen (1S28918N and 1S29220N).

Conflict of interest

L.L. has received a travel grant from Oxford Nanopore Technologies (ONT) to present his findings at a scientific meeting.

Acknowledgements

We would like to acknowledge and thank all participants who donated samples and all the clinicians and study nurses that assisted with the sample collection. We are grateful for the discussions with and input from Sarah Palmer, Bethany Horsburgh and Søren Karst. In addition, we would like to thank Ellen De Meester, Sarah De Keulenaer, and Sylvie Decraene from NXTGNT for their assistance in performing MiSeq sequencing. The following reagents were obtained through the NIH HIV Reagent Program, Division of AIDS, NIAID, NIH: J-Lat Full Length Cells (8.4), ARP-9847, contributed by Dr. Eric Verdin and Jurkat (E6-1) Cells, ARP-177, contributed by ATCC (Dr. Arthur Weiss).

References

1. Finzi,D., Hermankova,M., Pierson,T., Carruth,L.M., Buck,C., Chaisson,R.E., Quinn,T.C., Chadwick,K., Margolick,J., Brookmeyer,R., *et al.* (1997) Identification of a reservoir for HIV-1 in patients on highly active antiretroviral therapy. *Science*, **278**, 1295–1300.

2. Wong,J.K., Hezareh,M., Günthard,H.F., Havlir,D.V., Ignacio,C.C., Spina,C.A. and Richman,D.D. (1997) Recovery of Replication-Competent HIV Despite Prolonged Suppression of Plasma Viremia. *Science*, **278**, 1291–1295.

3. Chun,T.W., Engel,D., Berrey,M.M., Shea,T., Corey,L. and Fauci,A.S. (1998) Early establishment of a pool of latently infected, resting CD4(+) T cells during primary HIV-1 infection. *Proc Natl Acad Sci U S A*, **95**, 8869–8873.

4. Finzi,D., Blankson,J., Siliciano,J.D., Margolick,J.B., Chadwick,K., Pierson,T., Smith,K., Lisziewicz,J., Lori,F., Flexner,C., *et al.* (1999) Latent infection of CD4+ T cells provides a mechanism for lifelong persistence of HIV-1, even in patients on effective combination therapy. *Nat Med*, **5**, 512–517.

5. Chun,T.-W., Justement,J.S., Murray,D., Hallahan,C.W., Maenza,J., Collier,A.C., Sheth,P.M., Kaul,R., Ostrowski,M., Moir,S., *et al.* (2010) Rebound of plasma viremia following cessation of antiretroviral therapy despite profoundly low levels of HIV reservoir: implications for eradication. *AIDS*, **24**, 2803–2808.

6. Davey,R.T., Bhat,N., Yoder,C., Chun,T.-W., Metcalf,J.A., Dewar,R., Natarajan,V., Lempicki,R.A., Adelsberger,J.W., Miller,K.D., *et al.* (1999) HIV-1 and T cell dynamics after interruption of highly active antiretroviral therapy (HAART) in patients with a history of sustained viral suppression. *Proc Natl Acad Sci U S A*, **96**, 15109–15114.

7. Eriksson,S., Graf,E.H., Dahl,V., Strain,M.C., Yukl,S.A., Lysenko,E.S., Bosch,R.J., Lai,J., Chioma,S., Emad,F., *et al.* (2013) Comparative Analysis of Measures of Viral Reservoirs in HIV-1 Eradication Studies. *PLOS Pathogens*, **9**, e1003174.

8. Siliciano,J.D., Kajdas,J., Finzi,D., Quinn,T.C., Chadwick,K., Margolick,J.B., Kovacs,C., Gange,S.J. and Siliciano,R.F. (2003) Long-term follow-up studies confirm the stability of the latent reservoir for HIV-1 in resting CD4+ T cells. *Nat Med*, **9**, 727–728.

9. Deeks,S.G., Archin,N., Cannon,P., Collins,S., Jones,R.B., de Jong,M.A.W.P., Lambotte,O., Lamplough,R., Ndung'u,T., Sugarman,J., *et al.* (2021) Research priorities for an HIV cure: International AIDS Society Global Scientific Strategy 2021. *Nat Med*, **27**, 2085–2098.

10. Lambrechts,L., Cole,B., Rutsaert,S., Trypsteen,W. and Vandekerckhove,L. (2020) Emerging PCR-Based Techniques to Study HIV-1 Reservoir Persistence. *Viruses*, **12**, 149.

11. Crooks,A.M., Bateson,R., Cope,A.B., Dahl,N.P., Griggs,M.K., Kuruc,J.D., Gay,C.L., Eron,J.J., Margolis,D.M., Bosch,R.J., *et al.* (2015) Precise Quantitation of the Latent HIV-1 Reservoir: Implications for Eradication Strategies. *J Infect Dis*, **212**, 1361–1365.

12. Lorenzi,J.C.C., Cohen,Y.Z., Cohn,L.B., Kreider,E.F., Barton,J.P., Learn,G.H., Oliveira,T., Lavine,C.L., Horwitz,J.A., Settler,A., *et al.* (2016) Paired quantitative and qualitative assessment of the replication-competent HIV-1 reservoir and comparison with integrated proviral DNA. *Proc Natl Acad Sci U S A*, **113**, E7908–E7916.

13. Palmer,S., Kearney,M., Maldarelli,F., Halvas,E.K., Bixby,C.J., Bazmi,H., Rock,D., Falloon,J., Davey,R.T., Dewar,R.L., *et al.* (2005) Multiple, Linked Human Immunodeficiency Virus Type 1 Drug Resistance Mutations in Treatment-Experienced Patients Are Missed by Standard Genotype Analysis. *J Clin Microbiol*, **43**, 406–413.

14. Josefsson,L., Palmer,S., Faria,N.R., Lemey,P., Casazza,J., Ambrozak,D., Kearney,M., Shao,W., Kottilil,S., Sneller,M., *et al.* (2013) Single Cell Analysis of Lymph Node Tissue from HIV-1 Infected Patients Reveals that the Majority of CD4+ T-cells Contain One HIV-1 DNA Molecule. *PLoS Pathog*, **9**.

15. Ho,Y.-C., Shan,L., Hosmane,N.N., Wang,J., Laskey,S.B., Rosenbloom,D.I.S., Lai,J., Blankson,J.N., Siliciano,J.D. and Siliciano,R.F. (2013) Replication-competent noninduced proviruses in the latent reservoir increase barrier to HIV-1 cure. *Cell*, **155**, 540–51.

16. Bruner,K.M., Murray,A.J., Pollack,R.A., Soliman,M.G., Laskey,S.B., Capoferri,A.A., Lai,J., Strain,M.C., Lada,S.M., Hoh,R., *et al.* (2016) Defective proviruses rapidly accumulate during acute HIV-1 infection. *Nature medicine*, **22**, 1043–9.

17. Hiener,B., Horsburgh,B.A., Eden,J.-S., Barton,K., Schlub,T.E., Lee,E., von Stockenstrom,S., Odevall,L., Milush,J.M., Liegler,T., *et al.* (2017) Identification of Genetically Intact HIV-1 Proviruses in Specific CD4+ T Cells from Effectively Treated Participants. *Cell reports*, **21**, 813–822.

18. Lee,G.Q., Orlova-Fink,N., Einkauf,K., Chowdhury,F.Z., Sun,X., Harrington,S., Kuo,H.H., Hua,S., Chen,H.R., Ouyang,Z., *et al.* (2017) Clonal expansion of genome-intact HIV-1 in functionally polarized Th1 CD4+T cells. *Journal of Clinical Investigation*, **127**.

19. Pinzone,M.R., VanBelzen,D.J., Weissman,S., Bertuccio,M.P., Cannon,L., Venanzi-Rullo,E., Migueles,S., Jones,R.B., Mota,T., Joseph,S.B., *et al.* (2019) Longitudinal HIV sequencing reveals reservoir expression leading to decay which is obscured by clonal expansion. *Nat Commun*, **10**, 728.

20. Cole,B., Lambrechts,L., Gantner,P., Noppe,Y., Bonine,N., Witkowski,W., Chen,L., Palmer,S., Mullins,J.I., Chomont,N., *et al.* (2021) In-depth single-cell analysis of translation-competent HIV-1 reservoirs identifies cellular sources of plasma viremia. *Nat Commun*, **12**, 3727.

21. Sannier,G., Dubé,M., Dufour,C., Richard,C., Brassard,N., Delgado,G.-G., Pagliuzza,A., Baxter,A.E., Niessl,J., Brunet-Ratnasingham,E., *et al.* (2021) Combined single-cell transcriptional, translational, and genomic profiling reveals HIV-1 reservoir diversity. *Cell Reports*, **36**, 109643.

22. Gantner,P., Buranapraditkun,S., Pagliuzza,A., Dufour,C., Pardons,M., Mitchell,J.L., Kroon,E., Sacdalan,C., Tulmethakaan,N., Pinyakorn,S., *et al.* (2022) HIV rapidly targets a diverse pool of CD4+ T cells to establish productive and latent infections. 10.1101/2022.05.10.491275.

23. Lee,G.Q. (2021) Chemistry and Bioinformatics Considerations in Using Next-Generation Sequencing Technologies to Inferring HIV Proviral DNA Genome-Intactness. *Viruses*, **13**, 1874.

24. Shendure,J., Balasubramanian,S., Church,G.M., Gilbert,W., Rogers,J., Schloss,J.A. and Waterston,R.H. (2017) DNA sequencing at 40: past, present and future. *Nature*, **550**, 345–353.

25. Karst,S.M., Ziels,R.M., Kirkegaard,R.H., Sørensen,E.A., McDonald,D., Zhu,Q., Knight,R. and Albertsen,M. (2021) High-accuracy long-read amplicon sequences using unique molecular identifiers with Nanopore or PacBio sequencing. *Nat Methods*, **18**, 165–169.

26. Jordan,A., Bisgrove,D. and Verdin,E. (2003) HIV reproducibly establishes a latent infection after acute infection of T cells in vitro. *EMBO J*, **22**, 1868–1877.

27. Weiss,A., Wiskocil,R.L. and Stobo,J.D. (1984) The role of T3 surface molecules in the activation of human T cells: a two-stimulus requirement for IL 2 production reflects events occurring at a pre-translational level. *J Immunol*, **133**, 123–128.

28. Rutsaert,S., De Spiegelaere,W., De Clercq,L. and Vandekerckhove,L. (2019) Evaluation of HIV-1 reservoir levels as possible markers for virological failure during boosted darunavir monotherapy. *Journal of Antimicrobial Chemotherapy*, **74**, 3030–3034.

29. Trypsteen,W., Vynck,M., De Neve,J., Bonczkowski,P., Kiselinova,M., Malatinkova,E., Vervisch,K., Thas,O., Vandekerckhove,L. and De Spiegelaere,W. (2015) ddpcRquant: threshold determination for single channel droplet digital PCR experiments. *Anal Bioanal Chem*, **407**, 5827–5834.

30. Martin,M. (2011) Cutadapt removes adapter sequences from high-throughput sequencing reads. *EMBnet.journal*, **17**, 10–12.

31. Edgar,R.C. (2010) Search and clustering orders of magnitude faster than BLAST. *Bioinformatics*, **26**, 2460–2461.

32. Li,H. (2018) Minimap2: pairwise alignment for nucleotide sequences. *Bioinformatics*, **34**, 3094–3100.

33. Vaser,R., Sović,I., Nagarajan,N. and Šikić,M. (2017) Fast and accurate de novo genome assembly from long uncorrected reads. *Genome Res*, **27**, 737–746.

34. MEGAHIT: an ultra-fast single-node solution for large and complex metagenomics assembly via succinct de Bruijn graph | Bioinformatics | Oxford Academic.

35. Altschul,S.F., Gish,W., Miller,W., Myers,E.W. and Lipman,D.J. (1990) Basic local alignment search tool. *Journal of Molecular Biology*, **215**, 403–410.

36. Katoh,K., Misawa,K., Kuma,K. and Miyata,T. (2002) MAFFT: a novel method for rapid multiple sequence alignment based on fast Fourier transform. *Nucleic Acids Res*, **30**, 3059–3066.

37. Deng,W., Maust,B.S., Nickle,D.C., Learn,G.H., Liu,Y., Heath,L., Kosakovsky Pond,S.L. and Mullins,J.I. (2010) DIVEIN: a web server to analyze phylogenies, sequence divergence, diversity, and informative sites. *Biotechniques*, **48**, 405–408.

38. Guindon,S., Dufayard,J.-F., Lefort,V., Anisimova,M., Hordijk,W. and Gascuel,O. (2010) New Algorithms and Methods to Estimate Maximum-Likelihood Phylogenies: Assessing the Performance of PhyML 3.0. *Systematic Biology*, **59**, 307–321.

39. R Core Team R: A Language and Environment for Statistical Computing R Foundation for Statistical Computing, Vienna, Austria.

40. Hadley,W. (2016) ggplot2: Elegant Graphics for Data Analysis Springer-Verlag New York.

41. Yu,G. (2020) Using ggtree to Visualize Data on Tree-Like Structures. *Curr Protoc Bioinformatics*, **69**, e96.

42. Pollack,R.A., Jones,R.B., Pertea,M., Bruner,K.M., Martin,A.R., Thomas,A.S., Capoferri,A.A., Beg,S.A., Huang,S.-H., Karandish,S., *et al.* (2017) Defective HIV-1 proviruses are expressed and can be recognized by cytotoxic T lymphocytes which shapes the proviral landscape. *Cell Host Microbe*, **21**, 494-506.e4.

43. White,J.A., Wu,F., Yasin,S., Moskovljevic,M., Varriale,J., Dragoni,F., Contreras,A.C., Duan,J., Zheng,M.Y., Tadzong,N.F., *et al.* (2023) Clonally expanded HIV-1 proviruses with 5'-Leader defects can give rise to nonsuppressible residual viremia. *J Clin Invest*, 10.1172/JCI165245.

44. Lewinski,M.K., Bisgrove,D., Shinn,P., Chen,H., Hoffmann,C., Hannenhalli,S., Verdin,E., Berry,C.C., Ecker,J.R. and Bushman,F.D. (2005) Genome-wide analysis of chromosomal features repressing human immunodeficiency virus transcription. *J Virol*, **79**, 6610–6619.

45. Einkauf,K.B., Osborn,M.R., Gao,C., Sun,W., Sun,X., Lian,X., Parsons,E.M., Gladkov,G.T., Seiger,K.W., Blackmer,J.E., *et al.* (2022) Parallel analysis of transcription, integration, and sequence of single HIV-1 proviruses. *Cell*, **185**, 266-282.e15.

46. Mendoza,P., Gruell,H., Nogueira,L., Pai,J.A., Butler,A.L., Millard,K., Lehmann,C., Suárez,I., Oliveira,T.Y., Lorenzi,J.C.C., *et al.* (2018) Combination therapy with anti-HIV-1 antibodies maintains viral suppression. *Nature*, **561**, 479–484.

47. Liu,B., Zhang,W., Xia,B., Jing,S., Du,Y., Zou,F., Li,R., Lu,L., Chen,S., Li,Y., *et al.* (2021) Broadly neutralizing antibody–derived CAR T cells reduce viral reservoir in individuals infected with HIV-1. *J Clin Invest*, **131**.

48. Gunst,J.D., Pahus,M.H., Rosás-Umbert,M., Lu,I.-N., Benfield,T., Nielsen,H., Johansen,I.S., Mohey,R., Østergaard,L., Klastrup,V., *et al.* (2022) Early intervention with 3BNC117 and romidepsin at antiretroviral treatment initiation in people with HIV-1: a phase 1b/2a, randomized trial. *Nat Med*, **28**, 2424–2435.

49. Artesi,M., Hahaut,V., Cole,B., Lambrechts,L., Ashrafi,F., Marçais,A., Hermine,O., Griebel,P., Arsic,N., van der Meer,F., *et al.* (2021) PCIP-seq: simultaneous sequencing of integrated viral genomes and their insertion sites with long reads. *Genome Biology*, **22**, 97.

50. Wright,I.A., Delaney,K.E., Katusiime,M.G.K., Botha,J.C., Engelbrecht,S., Kearney,M.F. and van Zyl,G.U. (2021) NanoHIV: A Bioinformatics Pipeline for Producing Accurate, Near Full-Length HIV Proviral Genomes Sequenced Using the Oxford Nanopore Technology. *Cells*, **10**, 2577.

51. Laird Smith,M., Murrell,B., Eren,K., Ignacio,C., Landais,E., Weaver,S., Phung,P., Ludka,C., Hepler,L., Caballero,G., *et al.* (2016) Rapid Sequencing of Complete env Genes from Primary HIV-1 Samples. *Virus Evol*, **2**, vew018.

690 52. Gallardo,C.M., Wang,S., Montiel-Garcia,D.J., Little,S.J., Smith,D.M., Routh,A.L. and
691 Torbett,B.E. (2021) MrHAMER yields highly accurate single molecule viral
692 sequences enabling analysis of intra-host evolution. *Nucleic Acids Research*, **49**,
693 e70.

694 53. Sze,M.A. and Schloss,P.D. (2019) The Impact of DNA Polymerase and Number of
695 Rounds of Amplification in PCR on 16S rRNA Gene Sequence Data. *mSphere*, **4**,
696 e00163-19.

697

Table and Figure Legends

Figure 1 HIV-PULSE methodology overview and performance evaluation. (A) Schematic overview of the HIV-PULSE assay. A PCR reaction with bulk DNA containing multiple HIV-1 templates is pre-amplified using outer HIV-1 primers for a limited number of cycles to improve sensitivity. Next, pre-amplified material is tagged with a dual barcode consisting of a unique molecular identifier (UMI) attached to both ends using an HIV-1 specific inner primer. To generate enough material for long-read library preparation, the tagged material is amplified with synthetic primers in several PCR rounds followed by clean up to prevent length bias. (B) Success rate of the HIV-PULSE assay for different input ratios of HIV-1 with varying number of PCR cycles during pre-amplification. Each condition was performed in triplicate. (C) Mean accuracy of HIV-PULSE bin consensus sequences with increasing bin coverage compared to the Illumina reference sequence. The dashed line indicates the Q30 (99.9% accuracy) threshold. (D) Mean number of errors (insertions, deletions and mismatches) found in HIV-PULSE consensus sequences of 9.5 kb with increasing bin coverage compared to the Illumina reference sequence.

Figure 2 Benchmarking assays: novel HIV-PULSE vs gold standard FLIPS. (A) Donut plots displaying the fraction of unique and presumed clonal proviral sequences detected in each participant for both assays. The number of distinct proviruses generated by each assay is shown in the middle of each donut. The matching colored slices indicate the 6 out of 16 overlapping expansions of identical sequences (EIS) found to be clonal in both assays. p values test was used for a difference in the proportion of unique proviruses between both assays by ‘‘prop.test’’ in R, none were significant (p=1.00, p=0.583, p=1.00, p=1.00 for P03, P12_T1, P12_T2 and P14, respectively). (B) Size distributions of the observed proviral genome lengths for each assay. No significant difference was observed between both assays using a Kruskal-Wallis test (p= 0.08099). Each dot represents a single distinct provirus and is given a color for each participant. (C) For each assay and participant, the percentage of detected proviruses out of the total HIV-1 DNA reservoir size is shown.

Assay efficiencies were compared for significance using a Kruskal-Wallis test -test (p=0.248).

Figure 3 Proviral reservoir as assayed by the HIV-PULSE assay for a chronic cohort. (A) The proportions of different proviral classes observed among the distinct proviruses for each participant. On the right the number of total and distinct proviruses is displayed for each participant. (B) A phylogenetic tree including the distinct genome intact sequences. Each participant is shown as different colored dots, empty symbols indicate sequences only found once (unique, white insert) in a PCR replicate.

Figure 4 Benchmarking of HIV-PULSE vs STIP-Seq assay.

(A) Phylogenetic tree including all distinct proviruses obtained with the HIV-PULSE (excluding sequences with inversions, large deletions and hypermutations) and STIP-Seq assays for 8 participants. Symbols reflect the different assays, proviruses only recovered in a single assay are shown in grey while assay overlapping are shown in red (STIP-Seq) or blue (HIV-PULSE). Empty symbols indicate sequences were found once (unique, white insert) in that respective assay. The outer and inner circles indicate for each provirus respectively the participant origin and associated HIV-1 genome classification. (B) UpSet-plot visualizing the number of overlaps between clonal and unique proviruses recovered with each respective assays.

Supplemental Table 1 Clinical characteristics of chronic cohort participants.

Supplemental Table 2 List of primers used throughout the study.

Supplemental Table 3 Performance results of the HIV-PULSE assay on participants of a chronic cohort.

Supplemental Table 4 Estimated costs per sequenced virus for FLIPS and HIV-PULSE.

Supplemental Figure 1 HIV-PULSE assay details and performance.

(A) Visual presentation of the HIV-PULSE read construct layout. (B) Schematic representation of the bioinformatics workflow to analyze HIV-PULSE data. (C) Number of total reads for each HIV-PULSE sequencing run (LIB1 contained J-Lat 8.4 amplicon data, from LIB2 onwards clinical samples). (D) Sequencing library size (in base pairs) for each HIV-PULSE sequencing run. (E) Percentage of HIV-1 reads out of the total reads for each HIV-PULSE sequencing run. (F) Median read length of HIV-1 reads for each HIV-PULSE sequencing run. (G) Percentage of bins deemed correct out of the total detected bins for each HIV-PULSE sequencing run. (H) Percentage of reads belonging to correct bins out of the total number of binned reads for each HIV-PULSE sequencing run.

Supplemental Figure 2 Proviral reservoir as assayed by FLIPS.

(A) The proportions of different proviral classes observed among the distinct FLIPS proviruses for each participant. On the right the number of total and distinct proviruses, including proviruses that failed during *de novo* assembly is displayed for each participant (B) Distribution of the accuracy rates for all overlapping proviruses at different stages of the bioinformatics pipeline. The raw reads indicate the single-read accuracy (n= 232,131), racon3x and racon3x_medaka1x depict the HIV-PULSE bins (n=2,668) and megabins consists of the clustered HIV-PULSE bins (n=16). (C) Accuracy rates of overlapping proviruses detected with HIV-PULSE assay compared to their FLIPS Illumina reference counterpart. The color indicates the proviral genome classification by the HIV-PULSE assay for each respective provirus.

774 **Supplemental Figure 3 Bin coverage in function of amplicon length for all individuals**.
775 Each dot represents a single HIV-PULSE bin and is given a color based on the PCR-
776 replicate. The dashed red line indicates the Q30 (99.9%) bin accuracy threshold.

777

778 **Supplemental Figure 4 Comparison of longitudinal sequencing data for P12.**

779 Phylogenetic tree of HIV-PULSE proviruses from P12 sampled at different timepoints (3 year
780 interval). Tree was rooted against HXB2 and inversions were excluded (excluding 1 of the 21
781 timepoint overlapping clonal sequences). The symbols indicate the first (diamond) and
782 second (circle) sampling timepoint while colors indicate whether the provirus was detected
783 as clonal by the HIV-PULSE assay at that timepoint. The red arrows highlight identical
784 proviral sequences detected at both timepoints.

785 **Supplemental Figure 5 Correlation between the number of distinct HIV-1 proviruses**
786 **per PCR replicate and the total HIV-1 DNA reservoir size.**
787 For each participant, the number of distinct viruses for each sequenced PCR replicate are
788 shown with the averages indicated as empty circles. A Spearman correlation (R=0.71,
789 p=1.5*10^{15}) is made between the mean number of distinct and total HIV-1 DNA
790 copies/million CD4 cells as measured by ddPCR.

Figure 1

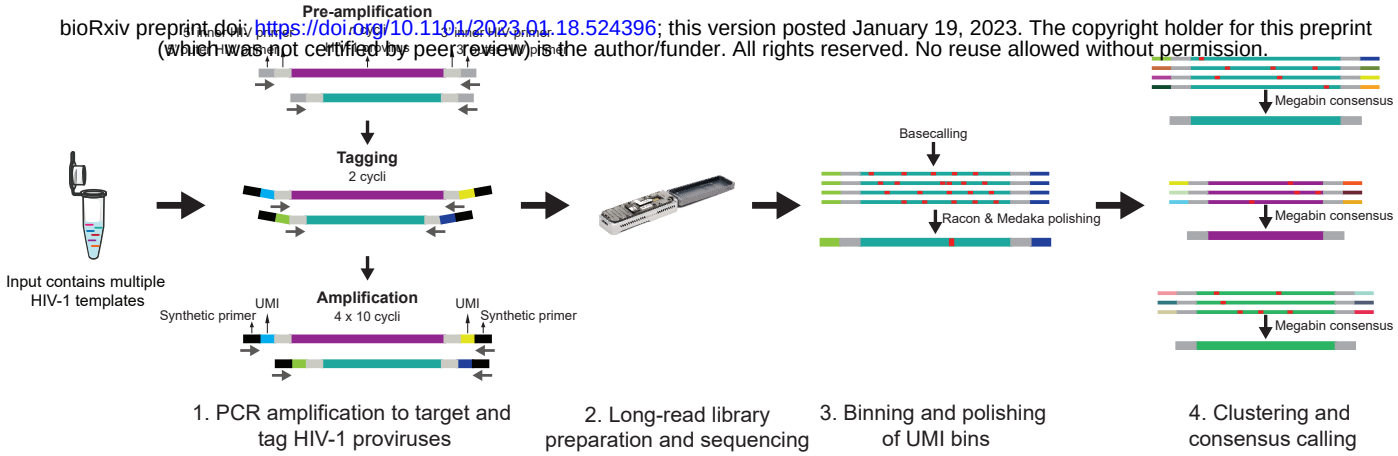

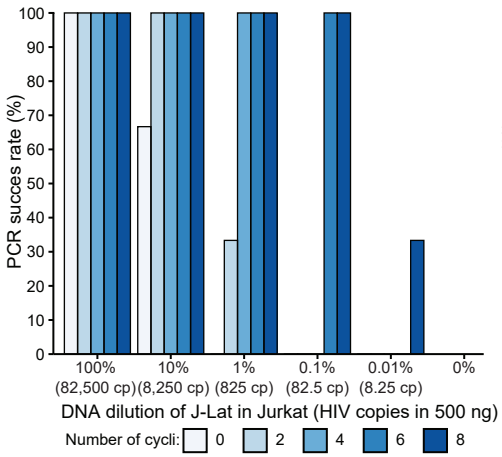

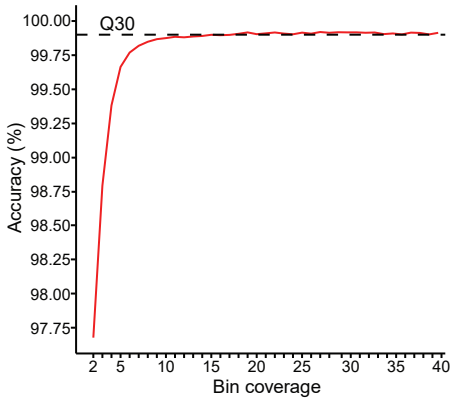

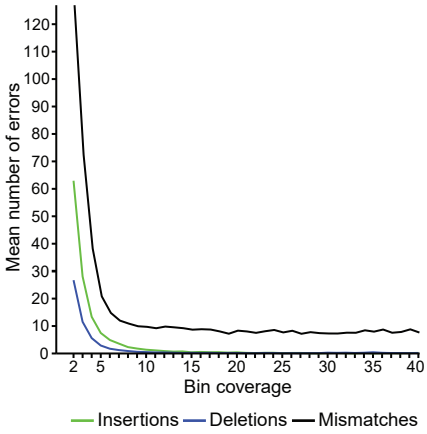

Figure 2

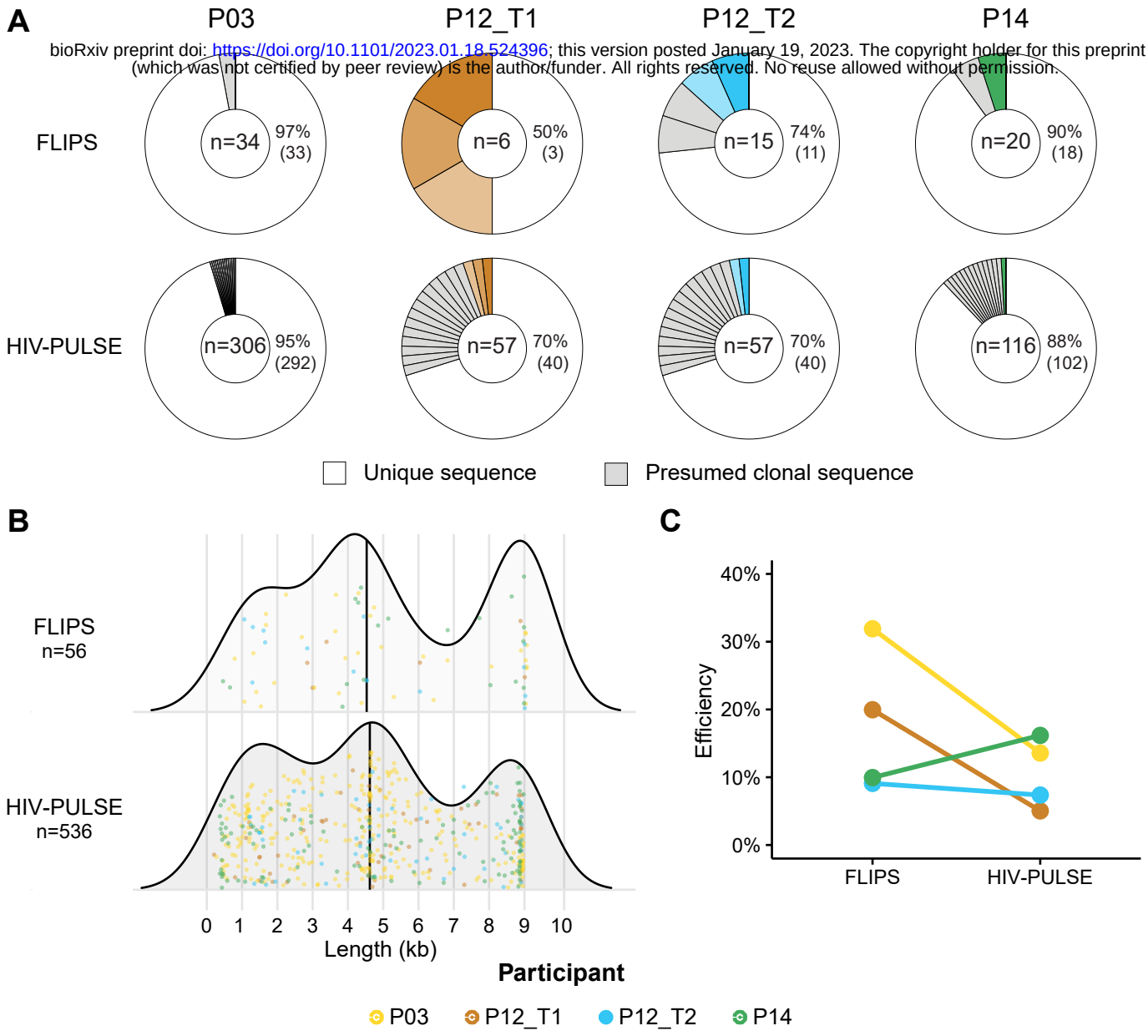

Figure 3

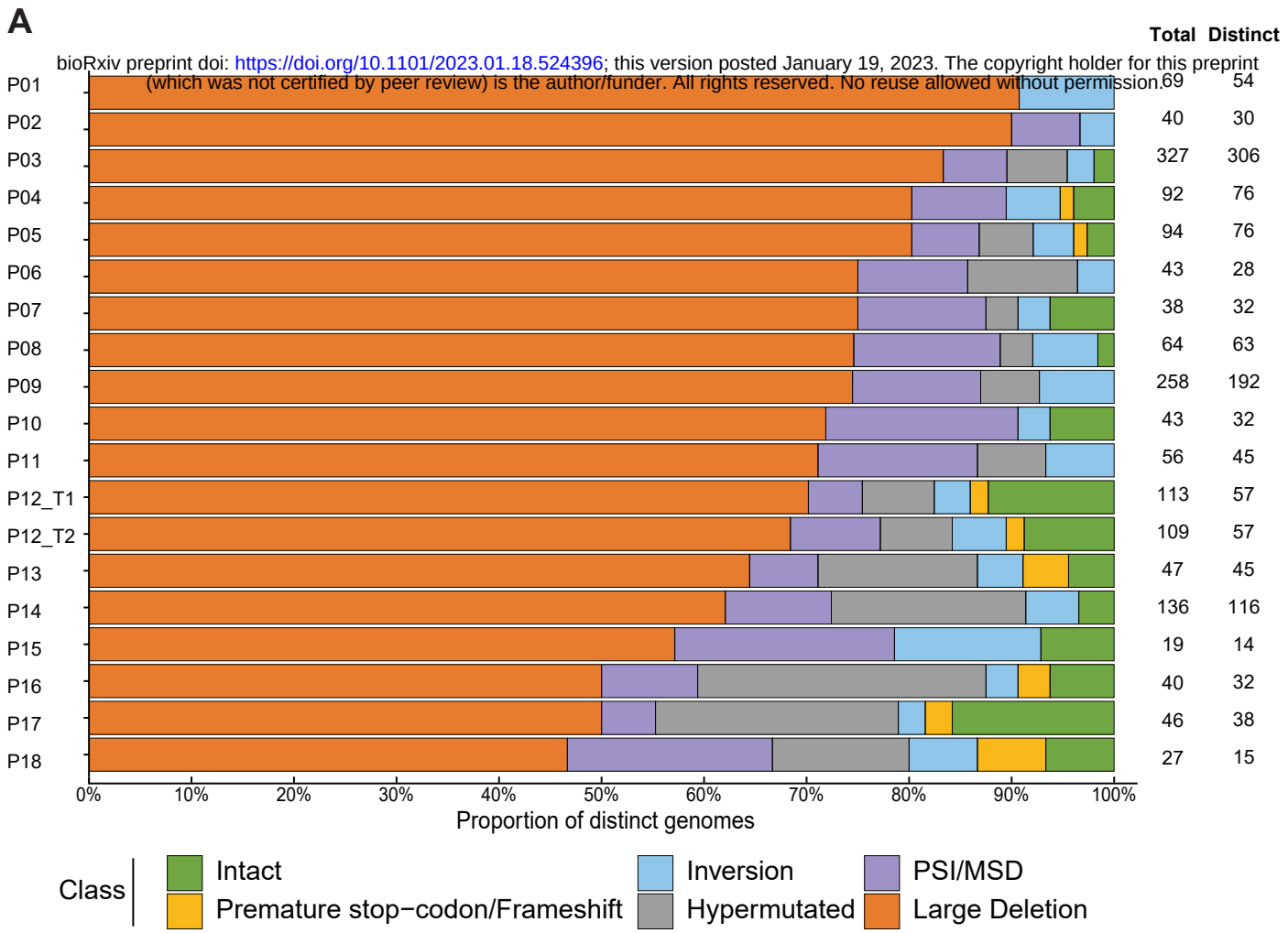

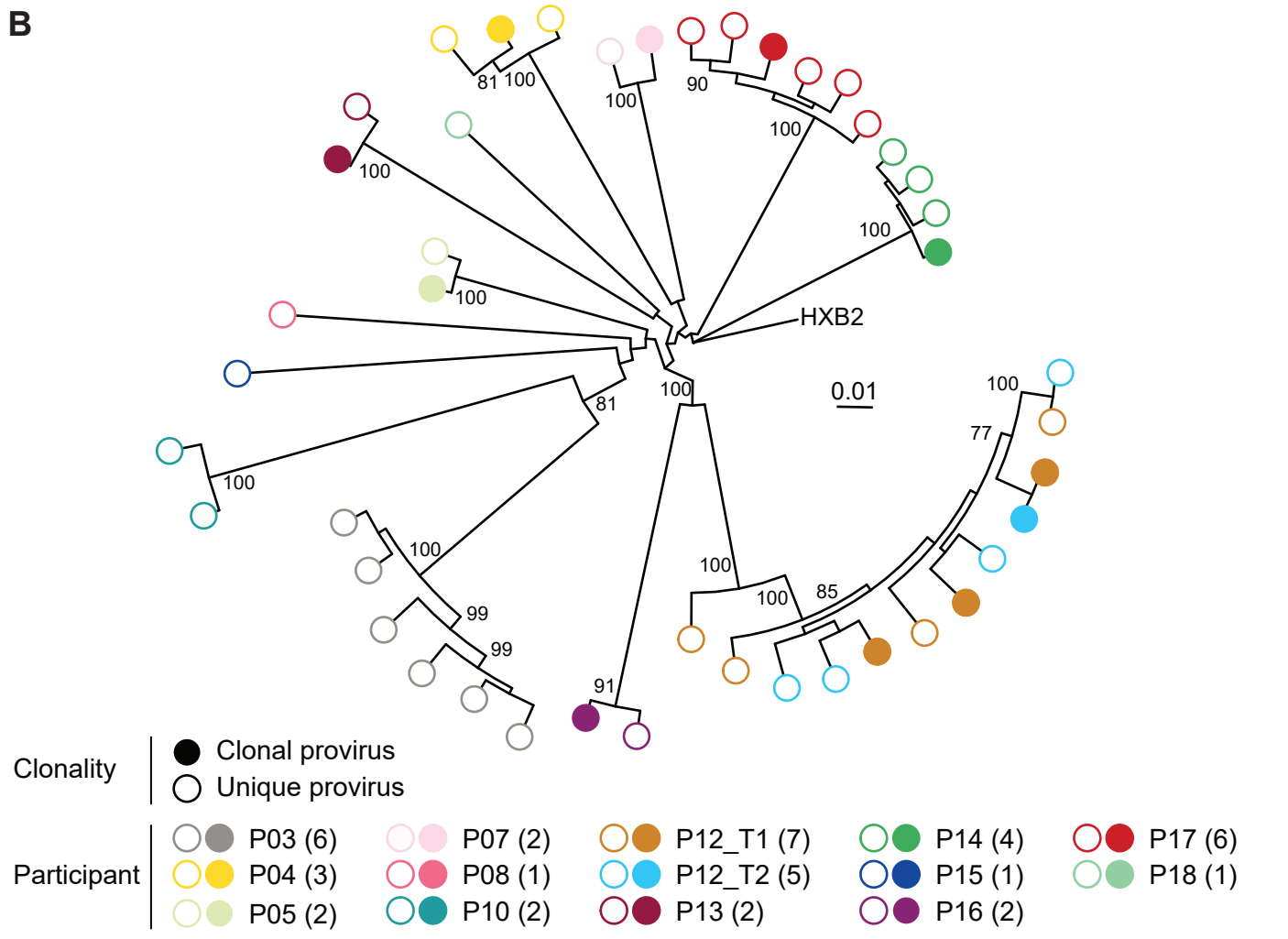

Figure 4

A

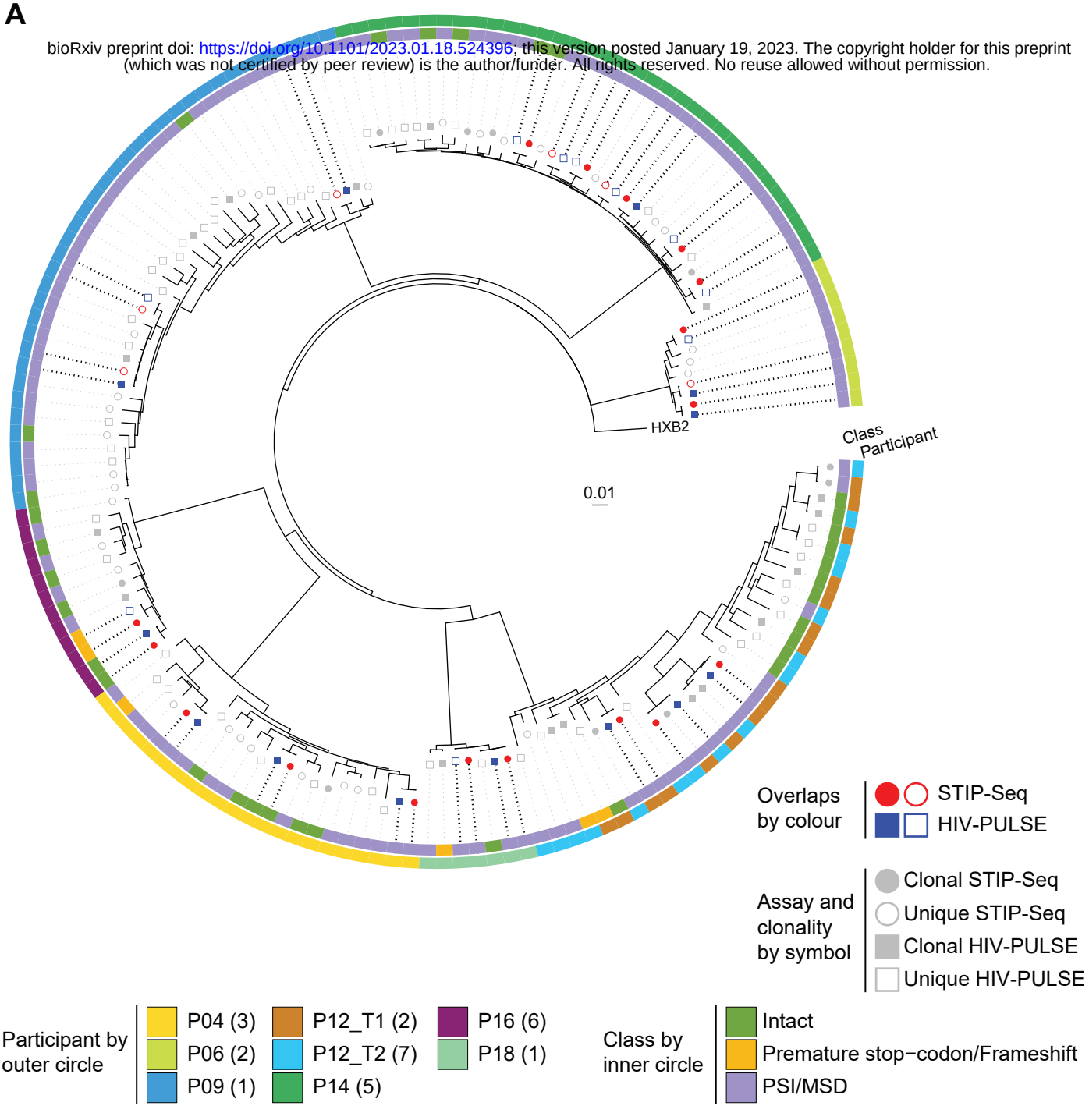

B